Homomeric Interaction of AtVSR1 Is Essential for Its Function as a Vacuolar Sorting Receptor[1][W][OA]

Hyeran Kim, Hyangju Kang, Mihue Jang, Jeong Ho Chang, Yansong Miao, Liwen Jiang, and Inhwan Hwang*

Division of Molecular and Life Sciences (H. Kim, H. Kang, M.J., J.H.C., I.H.) and Division of Integrative Biosciences and Biotechnology (I.H.), Pohang University of Science and Technology, Pohang 790–784, Korea; and Department of Biology and Molecular Biotechnology Program, Chinese University of Hong Kong, Shatin, New Territories, Hong Kong, China (Y.M., L.J.)

Vacuolar sorting receptors, BP80/VSRs, play a critical role in vacuolar trafficking of soluble proteins in plant cells. However, the mechanism of action of BP80 is not well understood. Here, we investigate the action mechanism of AtVSR1, a member of BP80 proteins in Arabidopsis (*Arabidopsis thaliana*), in vacuolar trafficking. AtVSR1 exists as multiple forms, including a high molecular mass homomeric complex in vivo. Both the transmembrane and carboxyl-terminal cytoplasmic domains of AtVSR1 are necessary for the homomeric interaction. The carboxyl-terminal cytoplasmic domain contains specific sequence information, whereas the transmembrane domain has a structural role in the homomeric interaction. In protoplasts, an AtVSR1 mutant, C2A, that contained alanine substitution of the region involved in the homomeric interaction, was defective in trafficking to the prevacuolar compartment and localized primarily to the trans-Golgi network. In addition, overexpression of C2A, but not wild-type AtVSR1, inhibited trafficking of soluble proteins to the vacuole and caused their secretion into the medium. Furthermore, C2A:hemagglutinin in transgenic plants interfered with the homomeric interaction of endogenous AtVSR1 and inhibited vacuolar trafficking of sporamin:green fluorescent protein. These data suggest that homomeric interaction of AtVSR1 is critical for its function as a vacuolar sorting receptor.

Newly synthesized organellar proteins are delivered to their respective organelles by a complex mechanism of transport. Vacuolar or secretory proteins are initially sorted and translocated into the endoplasmic reticulum (ER) cotranslationally (Crowley et al., 1994; Rapoport et al., 1996). After correct folding into a mature protein and assembly into complexes in the ER, these proteins are transported to the Golgi complex by COPII vesicles (Lee et al., 2004; Tang et al., 2005). Proteins that arrive nondiscriminantly to the Golgi complex are subject to sorting primarily at the trans-Golgi network (TGN), and depending on their final destination, they are transported to the prelysosomal or prevacuolar compartment (PVC; Harasaki et al., 2005; Traub, 2005). Lysosomal/vacuolar cargo-sorting receptors play a critical role in the sorting of cargoes at this step (Marcusson et al., 1994; Hadlington and Denecke, 2000; Gu et al., 2001; Tse et al., 2009).

In plant cells, the search for vacuolar sorting receptors led to the identification of an 80-kD protein called BP80 (Kirsch et al., 1994, 1996; Paris and Neuhaus, 2002). BP80 is a type I membrane protein and a member of a highly conserved family of proteins in plants termed vacuolar sorting receptors (VSRs; Kirsch et al., 1994, 1996; Ahmed et al., 1997). BP80/VSRs localize primarily to the PVC, with a minor portion located in the TGN (Sanderfoot et al., 1998; Li et al., 2002; Tse et al., 2004). Thus, it has been proposed that BP80/VSRs shuttle between the PVC and the TGN. In the TGN, they are involved in sorting of vacuolar proteins containing a vacuolar sorting motif, NPIR, for packaging into clathrin-coated vesicles (CCVs). In support of this theory, it was shown that in vitro, BP80/VSR binds to the N-terminal propeptide-sorting signal, the NPIR motif (Kirsch et al., 1994, 1996; Ahmed et al., 1997, 2000). In addition, overexpression of the ER-localized luminal domain of PV72, a seed-specific vacuolar sorting receptor, interferes with the transport of an NPIR-containing proteinase in Arabidopsis (*Arabidopsis thaliana*) leaves (Watanabe et al., 2004). The biological role of BP80/VSRs was demonstrated in protoplasts. Expression of a mutant form of BP80/VSR, in which the luminal domain was replaced

[1] This work was supported by grants from a national creative research program and the World Class University Project (project no. R31–2008–000–10105–0) of the Ministry of Science and Technology (Korea), the Technology Development Program for Agriculture and Forestry, Ministry for Food, Agriculture, Forestry, and Fisheries (grant no. 609004–05–1–SB210), and the BioGreen 21 Program, Rural Development Administration, Republic of Korea (grant no. 20100301–061–216–001–05–00).

* Corresponding author; e-mail ihhwang@postech.ac.kr.

The author responsible for distribution of materials integral to the findings presented in this article in accordance with the policy described in the Instructions for Authors (www.plantphysiol.org) is: Inhwan Hwang (ihhwang@postech.ac.kr).

[W] The online version of this article contains Web-only data.

[OA] Open Access articles can be viewed online without a subscription.

www.plantphysiol.org/cgi/doi/10.1104/pp.110.159814

with GFP, resulted in secretion of a soluble vacuolar protein, indicating that BP80/VSR functions in protein trafficking to the lytic vacuole (daSilva et al., 2005). In addition, recently it has been demonstrated that AtVSR1 plays a role in trafficking of protein storage vacuoles in plant seed cells (Shimada et al., 2003). In the *atvsr1* mutant, storage proteins were secreted into the apoplastic space of Arabidopsis seeds. In this case, the sorting signal recognized by AtVSR1 may be different from the NPIR motif found in proteins destined to the central vacuole.

Although there is mounting evidence that BP80/VSR functions as a vacuolar sorting receptor in plant cells (daSilva et al., 2005; Oliviusson et al., 2006), the detailed mechanism of its action remains poorly understood. Man-6-P receptors and Vps10p, the sorting receptors for soluble lysosomal and vacuolar hydrolases in animal and yeast, respectively, recruit adaptor proteins such as adaptor protein complex 1 (AP-1) and Golgi-localized, γ-ear-containing Arf-binding proteins using the C-terminal cytoplasmic domain (CCD; Johnson and Kornfeld, 1992; Dintzis et al., 1994; Honing et al., 1997; Seaman et al., 1997; Nothwehr et al., 2000; Puertollano et al., 2001; Dennes et al., 2002; Doray et al., 2002; Nakatsu and Ohno, 2003). Similarly, the CCD of BP80/VSR may also recruit accessory proteins for CCV formation at the TGN. Indeed, AtVSR1 interacts with EpsinR1 (formally EPSIN1), one of the epsin homologs in Arabidopsis (Song et al., 2006). Since EpsinR1 interacts with clathrin directly, this interaction may play a role in CCV formation. In addition, the CCD of BP80 contains a highly conserved sequence motif, YMPL, which conforms to the consensus sequence motif YXXΦ (where X is any amino acid and Φ is an amino acid with a bulky hydrophobic side chain) for binding to AP complexes. A peptide containing the YMPL motif binds in vitro to Arabidopsis μA, a close homolog of AP μ-adaptin in animal cells. The importance of the YXXΦ motif has also been confirmed by a recent study showing that mutation of the YXXΦ motif of BP80 caused its mistargeting in tobacco (*Nicotiana tabacum*) cells (daSilva et al., 2006). However, the exact role of the YXXΦ motif has not been addressed in trafficking of vacuolar proteins in vivo.

In an effort to understand the action mechanism of BP80/VSRs in plant cells, we examined the interaction of AtVSR1 with its binding partners. Here, we demonstrate that AtVSR1 undergoes homomeric interaction through the transmembrane domain (TMD) and CCD and that the homomeric interaction is critical for its function as sorting receptor of vacuolar proteins.

RESULTS

AtVSR1 Exists in Multiple Forms as Low and High Molecular Mass Complexes

To gain an insight into the action mechanism of AtVSR1, we examined the formation of AtVSR1 complexes in vivo. It has been suggested that the YXXΦ motif present in the CCD of AtVSR1 may interact with the μ subunit of the AP complex (Happel et al., 2004). Since multiple isoforms of highly homologous AtVSR exist in the cell and anti-VSR antibody recognized most of these isoforms (Miao et al., 2006), we generated transgenic plants with an epitope hemagglutinin (HA)-tagged AtVSR1, AtVSR1:HA, which allowed us to examine the behavior of AtVSR1 only. First, we fractionated protein extracts of leaf tissues by gel filtration column chromatography and analyzed these fractions by western blot using anti-HA antibody. The main peak of AtVSR1:HA eluted at a molecular mass of 240 kD, not at its size (80 kD), and a minor proportion at molecular mass greater than 240 kD (Fig. 1A). As controls for fractionation, binding protein (BiP), clathrin, and calreticulin were also monitored using their specific antibodies. BiP and calreticulin were detected at their expected positions, and clathrin was detected as high molecular mass forms (approximately 600 kD), as described previously (Kim et al., 2001). Triton X-100 is a nonionic detergent that often generates large aggregates, larger than 90,000 D, if concentration rises above 0.25 mM. To exclude the possibility that solubilization of membrane protein AtVSR1:HA with a buffer containing Triton X-100 may artificially increase the size of AtVSR1 by the formation of micelles, we performed gel filtration column chromatography again with CHAPS buffer. CHAPS is a zwitterionic detergent and can form smaller aggregates (6,000 D) even at the concentration of 10 mM. In the presence of CHAPS, the elution profile was slightly different from that obtained in the presence of Triton X-100. AtVSR1:HA was still eluted in a wide range of molecular masses, with two major peaks at 240 and 100 kD (Fig. 1B). At the same condition, BiP and clathrin were eluted at positions of 80 and 600 kD, respectively. These results raised the possibility that AtVSR1 exists in multiple forms, a high molecular mass complex and a monomeric form in vivo.

To test this further, we performed chemical cross-linking experiments. Fractions obtained from gel filtration column chromatography were divided into four groups, I, II, III, and IV (Fig. 1B), and subjected to chemical cross-linking using a water-soluble 3,3′-dithiobis[sulfosuccinimidylpropionate] (DTSSP) that reacts with primary amine groups. Subsequently, AtVSR1:HA was immunoprecipitated with anti-HA antibody and immunoprecipitates were analyzed by western blotting using anti-HA antibody. AtVSR1:HA produced two bands, one at 80 kD (one asterisk) and the other at approximately 240 kD (two asterisks; Fig. 1C, left). To confirm these results, we performed chemical cross-linking experiments using a different cross-linking reagent, dithiobis[succinimidylpropionate] (DSP), that is not sulfonated and thus not water soluble. DSP also reacts with primary amines to form covalent amide bonds. Proteins pooled from fractions 6 to 11 were subjected to chemical cross-linking and analyzed directly by western blotting using anti-HA

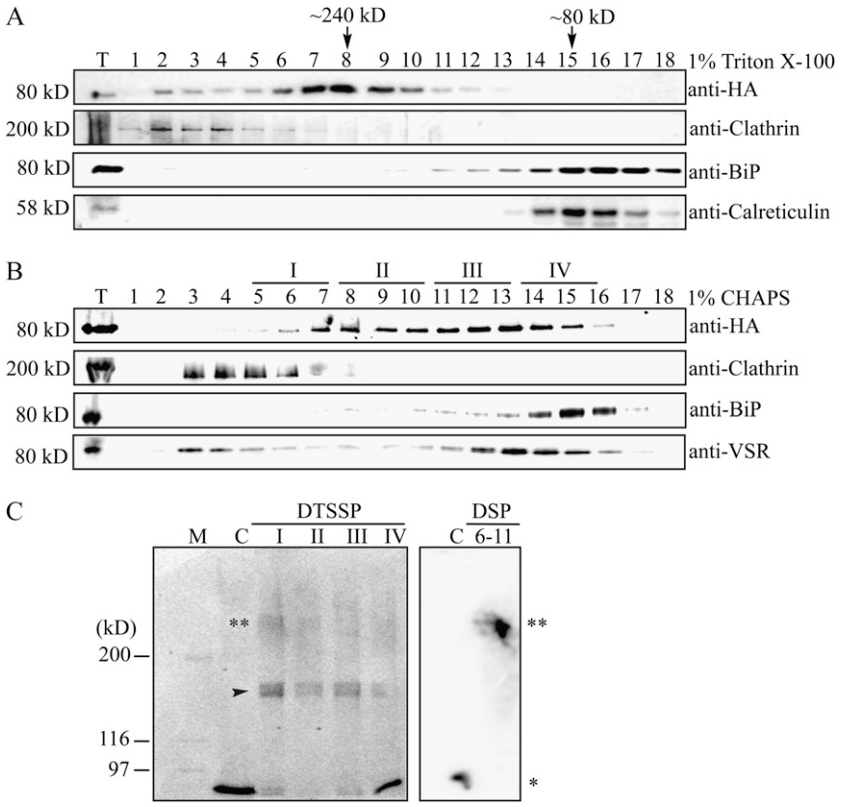

Figure 1. AtVSR1 exists as multiple forms: high molecular mass complex and monomeric form. A and B, Gel filtration column chromatography. Protein extracts were prepared from leaf tissues of transgenic plants expressing AtVSR1:HA and fractionated by gel filtration column chromatography using Superdex 200 HR 10/30. Protein extracts were solubilized by two different detergents, Triton X-100 (1%; A) and CHAPS (1%; B). Fractions were analyzed by western blot using the indicated antibodies. Molecular mass positions were determined using catalase (232 kD), bovine serum albumin (66 kD), and anti-clathrin antibody. T, Total protein extracts. C, Cross-linking of AtVSR1:HA. Fractions I, II, III, and IV indicated in B were pooled and subjected to chemical cross-linking as described in "Materials and Methods." Proteins that had been treated with DTSSP were subjected to immunoprecipitation with anti-HA antibody. The precipitates were boiled in a sample buffer without β-mercaptoethanol and separated on an SDS gel in the absence of β-mercaptoethanol, and AtVSR1:HA was detected by western-blot analysis using anti-HA antibody. In contrast, proteins that had been treated with DSP were directly detected by western blotting using anti-HA antibody. C, Total extracts that were boiled in a sample buffer containing β-mercaptoethanol but not treated with the chemical cross-linker; 6-11, fractions 6 to 11 that were pooled together for cross-linking experiments. Asterisks indicate the monomeric (*) and high molecular mass (**) forms. The arrowhead indicates IgG.

antibody. AtVSR1:HA was mainly detected as a high molecular mass form corresponding to 240 kD (Fig. 1C, right). These results clearly demonstrated that the high molecular mass form of AtVSR1:HA is not due to any abnormal mobility of AtVSR1:HA in the gel filtration column but due to complex formation of AtVSR1:HA in the cell.

AtVSR1 Undergoes Homomeric Interaction

To function as a vacuolar sorting receptor, AtVSR1 should interact with multiple proteins such as cargo proteins and AP complex (Ahmed et al., 2000; Shimada et al., 2003; Happel et al., 2004). However, we ruled out the possibility that the 240-kD form is a complex with cargo protein, because cargo proteins should have various molecular mass values. In addition, we ruled out the possibility that the 240-kD complex is composed of AtVSR1 and AP-1, because the molecular mass of μ-adaptin that directly interacts with a cargo-sorting receptor is approximately 50 kD and the whole AP-1 complex is around 275 kD. Thus, we explored the possibility of homomeric interaction of AtVSR1 molecules by a coimmunoprecipitation approach. We generated two differently tagged versions of AtVSR1, *AtVSR1:Myc* and *AtVSR1:HA*, and transiently expressed them in protoplasts from leaf tissues (Kim et al., 2005). Subsequently, protein extracts from transformed protoplasts were subjected to immunoprecipitation using anti-Myc antibody. AtVTI11:HA, which localizes to the TGN and the PVC (Zheng et al., 1999), was used as a negative control for the coimmunoprecipitation. The immunoprecipitates were analyzed by western blotting using anti-Myc and anti-HA antibodies. *R6*, the empty expression vector, was used as a control for immunoblot specificity. AtVSR1:HA was

detected in immune complexes obtained with anti-Myc antibody (Fig. 2A), indicating that AtVSR1:HA interacts with AtVSR1:Myc. In contrast, AtVTI11:HA was not detected in anti-Myc immunoprecipitates, confirming the specificity of the interaction. To confirm that the C-terminal epitopes do not contribute to the interaction, protoplasts were cotransformed with *AtVSR1:HA* and *GFP:AtVSR1*, and protein extracts were subjected to immunoprecipitation using anti-GFP antibody. GFP:AtVSR1, which had the luminal domain replaced with GFP, behaves similarly to the wild type in its localization (Miao et al., 2006). GFP alone was included as a negative control for GFP:AtVSR1. Immunoprecipitates were analyzed by western blotting using anti-HA and anti-GFP antibodies. AtVSR1:HA was detected in anti-GFP immune complexes from protoplasts expressing GFP:AtVSR1 but not GFP alone (Fig. 2B), confirming that a homomeric interaction occurs between AtVSR1 molecules.

Both the TMD and CCD Are Necessary for the Homomeric Interaction

To determine the domain(s) necessary for the homomeric interaction of AtVSR1, we generated several deletion and substitution mutants of AtVSR1 (Fig. 3A). These constructs were fused to Myc at their C termini. Myc-tagged deletion or substitution mutants were cotransformed into protoplasts together with *AtVSR1:HA*, and protein extracts were subjected to immunoprecipitation using anti-Myc antibody, followed by western-blot analysis using anti-HA and anti-Myc antibodies. Of AtVSR1 mutants, mutants that did not contain the TMD and unrelated CCD were not coimmunoprecipitated. Only the TS mutant that had the AtVSR1 TMD replaced with an unrelated TMD was coimmunoprecipitated with AtVSR1:HA (Fig. 3B). These results indicated that for homomeric interactions of AtVSR1, both the CCD and TMD are necessary but the TMD can be replaced with an unrelated one.

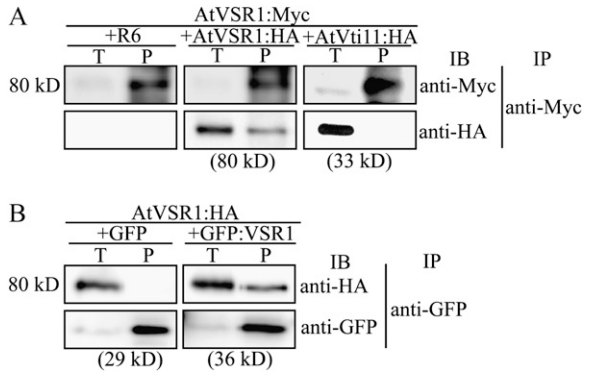

Figure 2. AtVSR1 undergoes homomeric interaction. Protoplasts were transformed with the indicated constructs, and protein extracts from transformed protoplasts were subjected to immunoprecipitation with anti-Myc (A) and anti-GFP (B) antibodies. Immunoprecipitates were analyzed by western blot using the indicated antibodies. AtVti11:HA (A) and GFP (B) were used as negative controls for AtVSR1:HA and GFP:VSR1 in coimmunoprecipitation experiments, respectively. IB, Immunoblot; IP, immunoprecipitation; P, immunoprecipitates; R6, the empty expression vector; T, total protein extracts (10% of input).

To further confirm these results, and to determine whether the homomeric interaction occurs directly between AtVSR1 molecules, we performed an in vitro pull-down experiment. A fragment containing the TMD and CCD was fused to maltose-binding protein (MBP), and subsequently, the fusion protein, MBP:TCT, was tagged with Myc or HA at its C terminus (MBP:TCT:HA/Myc). As a control, MBP was also tagged with Myc at its C terminus. These proteins were expressed in *Escherichia coli* and purified with amylose resin from *E. coli* extracts. Purified MBP:TCT:HA was incubated with MBP:Myc or MBP:TCT:Myc, and the mixtures were subjected to immunoprecipitation using anti-HA antibody. Immunoprecipitates were analyzed by western blotting using anti-HA and anti-Myc antibodies. We found that MBP:TCT:Myc, but not MBP:Myc, was present in anti-HA immunoprecipitates (Fig. 3C), indicating that the homomeric interaction is direct.

To identify the motif(s) involved in AtVSR1 homomeric interactions, we generated a series of mutants that had substitution of eight or nine amino acid residues with Ala residues. The mutants were fused to HA at their C termini (Fig. 4A). Ala substitution mutants were introduced into protoplasts together with *GFP:AtVSR1*, and protein extracts were subjected to immunoprecipitation using anti-GFP antibody. Immunoprecipitates were analyzed by western blotting using anti-HA and anti-GFP antibodies. The amount of C1A:HA and C4A:HA in anti-GFP immunoprecipitates was similar to that of AtVSR1 (Fig. 4B). In contrast, the amount of C2A:HA and C3A:HA in anti-GFP immunoprecipitates was reduced to 31% and 65% that of the wild type, respectively. These results demonstrated that both C2 and C3 segments contain sequence motifs for AtVSR1 homomeric interactions and that the motif in the C2 segment is the most critical. The C2 segment contained the critical Tyr residue of the YXXΦ motif, and the C3 segment contained the Φ residue of the YXXΦ motif. However, it is not clear whether this YXXΦ motif for the interaction with μ-adaptin is involved in the homomeric interaction of AtVSR1.

Homomeric AtVSR1 Complex Formation Is Critical for Its Role in Vacuolar Trafficking

To examine the significance of the homomeric AtVSR1 complex in its role as a vacuolar sorting receptor, protoplasts were cotransformed with *AALP:GFP* together with wild-type *AtVSR1:HA* or *C2A:HA*. Here, we used as a vacuolar cargo AALP:GFP, which is a chimeric protein consisting of Arabidopsis aleurain-like protein (AALP) and GFP and shown to be targeted to the central vacuole (Sohn et al., 2003). In protoplasts, AALP:GFP produces two protein species at 70 and

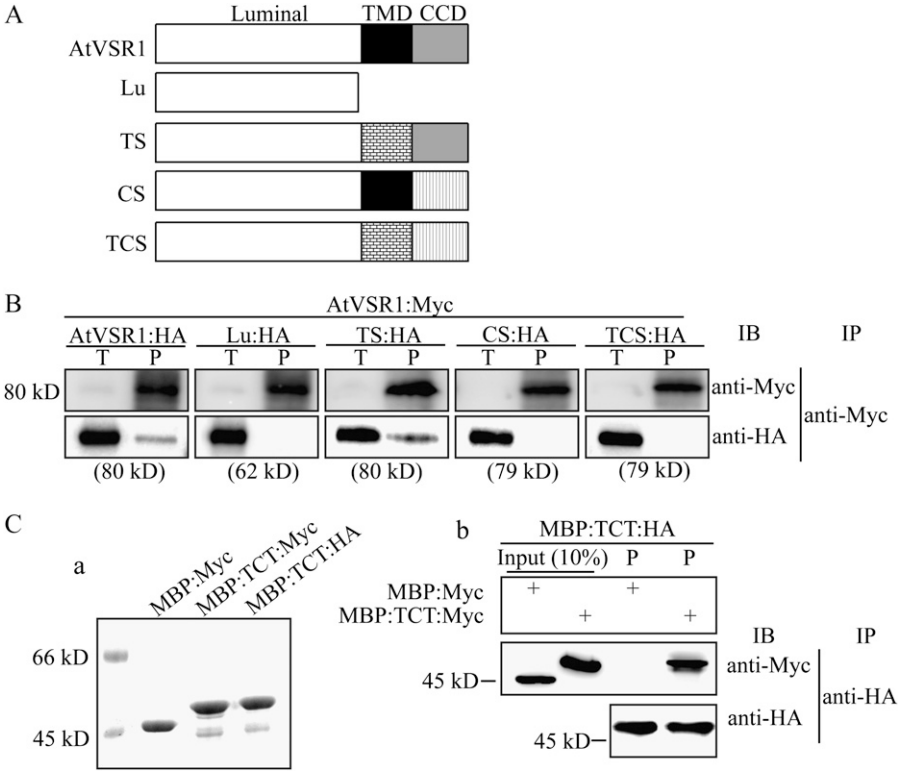

Figure 3. Both the TMD and CCD are necessary for the homomeric interaction of AtVSR1 molecules. A, Schemes of various AtVSR1 constructs. Lu contained the luminal domain only; TS contained a substitution of its TMD with the TMD of AtRMR1; CS contained a substitution of its CCD with the CCD (amino acid positions 193–310) of AtRMR1; TCS contained a substitution of both its TMD and CCD with the corresponding domains used to construct TS and CS. B, Coimmunoprecipitation of AtVSR1 deletion and substitution mutants. Protoplasts were transformed with the indicated constructs. Coimmunoprecipitation was performed as described in "Materials and Methods." IB, Immunoblot; IP, immunoprecipitation; P, immunoprecipitates; T, total protein extracts (10% of input). C, Protein pull-down experiment. An AtVSR1 fragment containing the TMD and CCD was fused to MBP. The fusion protein MBP:TCT was tagged with HA or Myc at the C terminus. The fusion proteins were purified from *E. coli* extracts (Coomassie Brilliant Blue-stained gel; panel a). Recombinant protein MBP:TCT:HA was incubated with MBP:TCT:Myc or MBP:Myc, and proteins were immunoprecipitated with anti-HA antibody. Immunoprecipitates were analyzed by western blot using anti-HA and anti-Myc antibodies (panel b). Input (10%), Ten percent of MBP:Myc or MBP:TCT:Myc used for the protein pull-down experiment.

30 kD when detected with anti-GFP antibody. The 70-kD species corresponds to the intact protein, and the 30-kD species is the processed form in the central vacuole. Thus, the amount of the 30-kD species can be used to measure vacuolar trafficking efficiency. Protein extracts from transformed protoplasts and incubation medium were analyzed by western blotting using anti-GFP antibody. In C2A:HA-expressing protoplasts, the amount of the processed 30-kD form of AALP:GFP was reduced, and a significant amount of AALP:GFP was secreted into the medium as early as 12 h post transformation, suggesting that C2A:HA inhibits trafficking of AALP:GFP to the central vacuole (Fig. 5A). In contrast, in the presence of wild-type AtVSR1:HA, vacuolar trafficking of AALP:GFP was not affected and AALP:GFP was not secreted into the medium. This result strongly suggested that C2A:HA inhibits vacuolar trafficking. We then examined the dose dependence of the cargo secretion, using increasing amounts of *C2A:HA* DNA. The amount of the 30-kD processed form was gradually decreased in a dose-dependent manner, and concomitantly, the amount of AALP:GFP secreted into medium was increased (Fig. 5, B and C).

To further confirm this result, we examined whether wild-type AtVSR1:HA can relieve the secretion effect of C2A:Myc. At 15 μg of *C2A:Myc*, *AtVSR1:HA* was introduced into protoplasts together with *AALP:GFP*. The total amount of plasmid DNA introduced was fixed at 30 μg. The amount of AALP:GFP secreted into medium was reduced when wild-type AtVSR1:HA was coexpressed together with C2A:Myc (Fig. 5D). These results strongly suggest that C2A competitively inhibits endogenous AtVSR1 in the vacuolar trafficking of AALP:GFP.

To obtain supporting evidence for the inhibitory effect of C2A:HA on the vacuolar trafficking, we used another vacuolar cargo, sporamin:GFP (Spo:GFP), a chimeric protein consisting of sporamin from sweet potato (*Ipomoea batatas*) and GFP (Kim et al., 2001), and

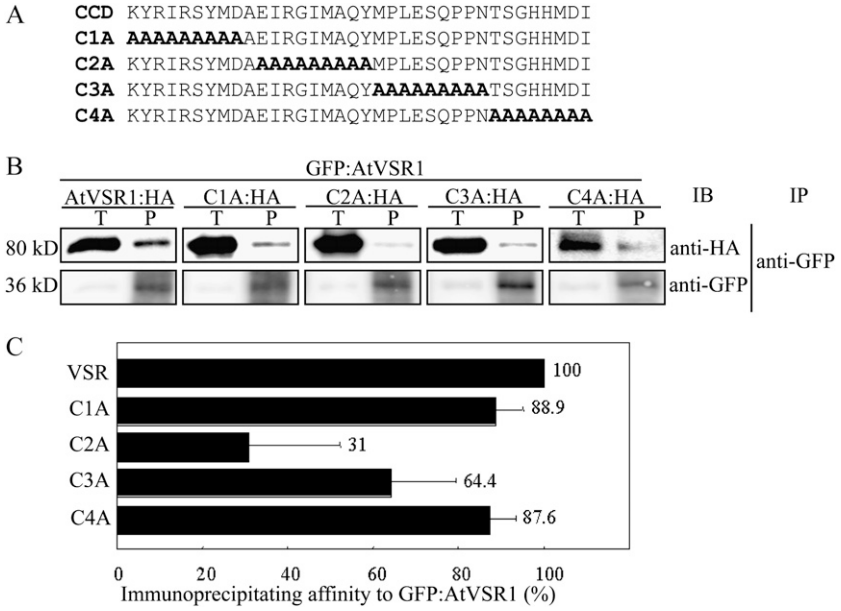

Figure 4. The C2 segment of the CCD is critical for homomeric interaction of AtVSR1. A, Sequences of Ala substitution mutants. The CCD region was divided into four regions, C1 to C4, and each region was substituted with Ala residues. B, Coimmunoprecipitation of AtVSR1 Ala substitution mutants. Protoplasts were transformed with the indicated constructs, and coimmunoprecipitation experiments were performed. IB, Immunoblot; IP, immunoprecipitation; P, immunoprecipitates; T, total protein extracts. C, Quantification of coimmunoprecipitation. The intensity of coimmunoprecipitated mutants was quantified using Multi Gauge analysis software and the LAS3000 image-capture system (FujiFilm) and was normalized by the input. The image of the blot was captured at many different exposure time points. For quantification, we selected images that yielded a linear relationship between the intensity and exposure time. To quantify the degree of coimmunoprecipitation, four independent immunoprecipitation experiments were performed. The numbers and error bars indicate the means and SD ($n = 4$), respectively.

examined its trafficking in the presence of C2A:HA in protoplasts. *Spo:GFP* was cotransformed into protoplasts together with *C2A:HA* or the empty expression vector *R6*, and protein extracts from the transformed protoplasts and incubation medium were analyzed by western blotting using anti-GFP antibody. In the presence of C2A:HA, the amount of 30-kD processed Spo:GFP was significantly reduced, and concomitantly, a portion of Spo:GFP was secreted into the medium (Fig. 5E), confirming that C2A:HA inhibits the trafficking of vacuolar proteins. In contrast to AALP:GFP, interestingly, Spo:GFP was proteolytically processed to a 30.5-kD form in the medium. Endogenous proteases secreted into the medium may be responsible for the processing. In previous studies, it has been shown that the proteolytic processing is largely dependent on individual proteins (Matsuoka et al., 1995; Frigerio et al., 1998; Sohn et al., 2003).

Next, to rule out the possibility that the secretion of AALP:GFP was caused by overexpression of C2A:HA, we examined the effect of C4A:HA, another mutant with Ala substitution at amino acid positions 616 to 623, on vacuolar trafficking of AALP:GFP. Varying amounts of *C4A:HA* were cotransformed into protoplasts together with *AALP:GFP*, and protein extracts from protoplasts and incubation medium were analyzed by western blotting using anti-GFP and anti-HA antibodies. At up to 30 μg of C4A:HA, AALP:GFP was not secreted into the incubation medium (Fig. 5F). These results strongly suggest that AALP:GFP secretion is specific to C2A:HA but not due to overexpression of AtVSR1.

C2A:HA Interferes with Homomeric Interaction of Endogenous AtVSR1 and Inhibits Vacuolar Trafficking of Spo:GFP in Transgenic Plants

Next, we examined the behavior of C2A:HA in planta and the effect of C2A:HA on the homomeric interaction of endogenous AtVSR. Transgenic plants were generated using C2A:HA. Initially, we examined the expression level of *C2A:HA* in the transgenic plants and compared it with that of the endogenous *AtVSR1* by reverse transcription (RT)-PCR. Total RNA was prepared from the wild type and two independent transgenic lines and subjected to RT-PCR using *C2A:HA*- or *AtVSR1*-specific primers. *C2A:HA* transcripts were severalfold higher in both transgenic lines than the endogenous *AtVSR1* transcript levels in wild-type plants (Fig. 6A). Another noticeable feature was that the expression of endogenous *AtVSR1* was greatly induced in C2A:HA transgenic plants as compared with the wild-type plants, which is not clearly understood at the moment. One possibility is that C2A:HA may act as a dominant negative mutant in the homomeric interaction and, thereby, expression of *C2A:HA*

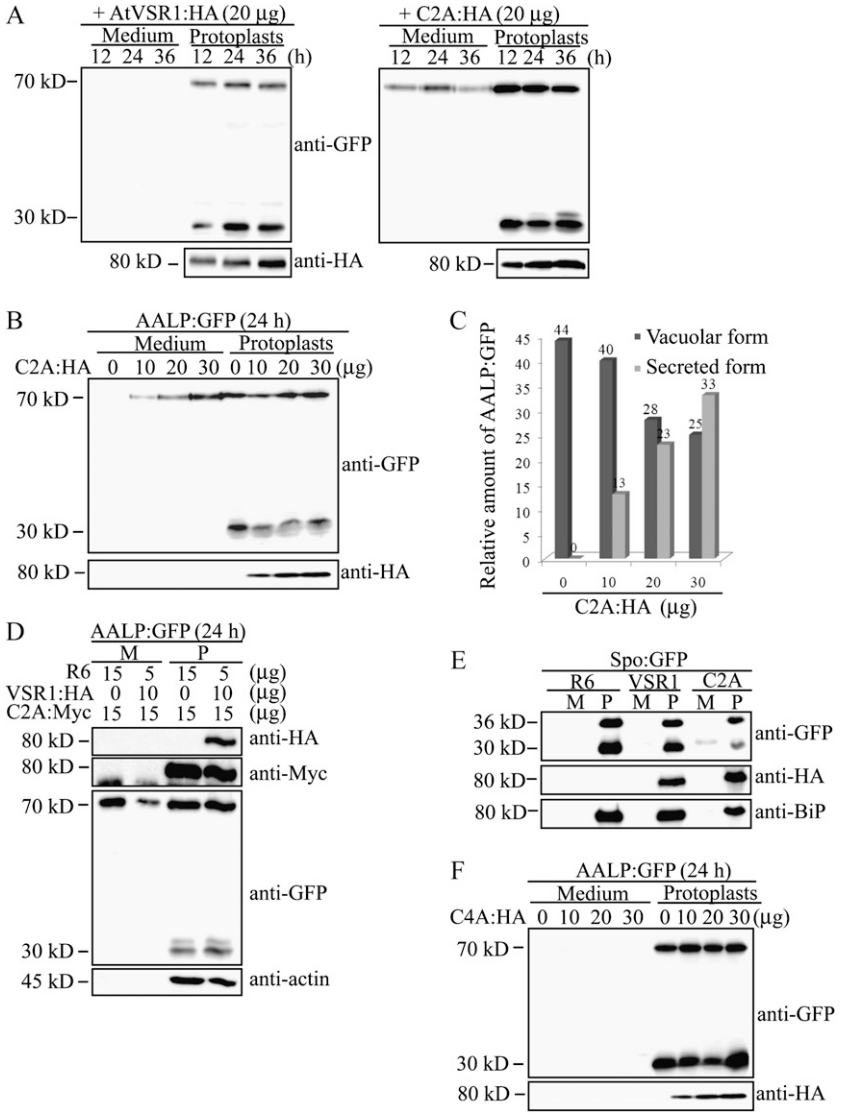

Figure 5. C2A:HA inhibits vacuolar trafficking of AALP:GFP and Spo:GFP in protoplasts. A, Inhibition of vacuolar trafficking of AALP:GFP by C2A:HA. Protoplasts were cotransformed with *AALP:GFP* (20 μg) together with *AtVSR1:HA* (20 μg) or *C2A:HA* (20 μg). Protein extracts were prepared from transformed protoplasts and incubation medium at the indicated time points after transformation and analyzed by western blot using anti-GFP and anti-HA antibodies. B, Dose-dependent inhibition of vacuolar trafficking of AALP:GFP by C2A:HA. Protoplasts were transformed with *AALP:GFP* together with the indicated amounts (μg) of *C2A:HA*. Trafficking of AALP:GFP was analyzed 24 h after transformation as described in A. C, Quantification of trafficking efficiency. To determine the trafficking efficiency, the intensity of bands shown in B was measured by software equipped with the LAS3000 image-capture system and expressed as relative values to the total amount of AALP:GFP (proteins in protoplasts and incubation medium). D, Suppression of C2A:HA-mediated vacuolar trafficking inhibition of AALP:GFP by wild-type AtVSR1. Protoplasts were transformed with the indicated constructs at the indicated amounts of DNA (μg). Protein extracts were prepared from transformed protoplasts and the incubation medium 24 h after transformation and analyzed by western blot using anti-HA, anti-GFP, anti-Myc, and anti-actin antibodies. Actin levels were used as a loading control. M, Incubation medium; P, protoplasts; R6, empty expression vector. E, Inhibition of vacuolar trafficking of Spo:GFP by C2A:HA. Protoplasts were cotransformed with *Spo:GFP* together with *AtVSR1:HA*, *C2A:HA*, or *R6*, and trafficking of Spo:GFP was examined by western-blot analysis using anti-GFP, anti-HA, and anti-BiP antibodies. Protein extracts were prepared from protoplasts and the incubation medium. BiP was detected as a control for protein leakage from protoplasts. F, C4A:HA does not affect trafficking of AALP:GFP to the vacuole. The indicated amount of *C4A:HA* that had Ala substitution from amino acid positions 616 to 623 was introduced into protoplasts together with *AALP:GFP*, and protein extracts from protoplasts and incubation medium were analyzed by western blotting using antibodies.

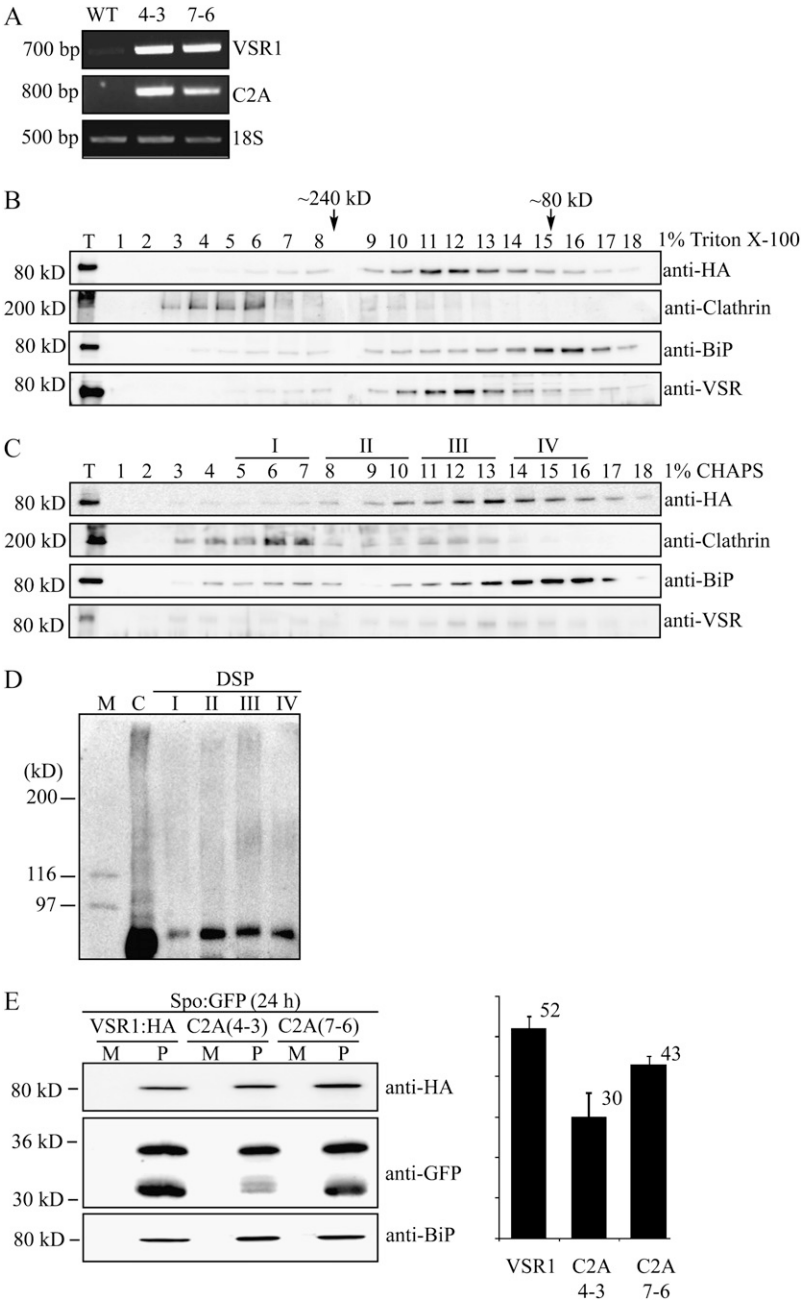

Figure 6. C2A:HA in transgenic plants interferes with the homomeric interaction of endogenous AtVSR1 and inhibits vacuolar trafficking of Spo:GFP. A, RT-PCR analysis of *C2A:HA* transcript levels in C2A:HA transgenic plants. Total RNA was prepared from the wild type (WT) and two independent transgenic lines (4-3 and 7-6), and the transcript levels of endogenous *AtVSR1* and *C2A:HA* were examined by RT-PCR analysis at the same condition using endogenous *AtVSR1*- and *C2A:HA*-specific primers. 18S rRNA was detected as an internal control. B and C, Gel filtration column chromatography. Protein extracts from leaf tissues of transgenic plants expressing C2A:HA were treated with Triton X-100 (1%; B) or CHAPS (1%; C) and fractionated by gel filtration column chromatography as described in Figure 1, A and B. Fractions were analyzed by western blot using the indicated antibodies. Molecular mass positions were determined using catalase (232 kD), bovine serum albumin (66 kD), and anti-clathrin antibody. T, Total protein extracts. D, Cross-linking of C2A:HA. Fractions I, II, III, and IV indicated in C were pooled and subjected to chemical cross-linking as described in "Materials and Methods." Proteins that had been treated with DSP were directly detected by western blotting using anti-HA antibody. C, Total protein extracts that were boiled in a sample buffer containing β-mercaptoethanol but not treated with the chemical cross-linker. E, Effect of C2A:HA expressed in transgenic plants on vacuolar trafficking of Spo:GFP. Protoplasts from two C2A:HA transgenic lines, C2A(4-3) and C2A(7-6), or AtVSR1:HA transgenic plants (VSR1) were transformed with *Spo:GFP*, and trafficking of Spo:GFP was examined by western-blot analysis using anti-HA, anti-GFP, and anti-BiP antibodies. To determine the trafficking efficiency, the intensity of the 30-kD processed form was quantified and expressed as a relative ratio to the total amount of Spo:GFP. BiP was detected as a control for protein leakage from protoplasts. M, Incubation medium; P, protoplasts.

in transgenic plants caused induction of the endogenous *AtVSR1* as a mechanism to counteract the dominant negative effect of C2A:HA.

To examine the behavior of C2A:HA in the transgenic plants, total proteins from C2A:HA transgenic plants were treated with Triton X-100 or CHAPS and separated by gel filtration column chromatography. These fractions were then analyzed by western blotting using anti-HA, anti-clathrin heavy chain, anti-BiP, and anti-VSR antibodies. The migration pattern of C2A:HA differed from that of AtVSR1:HA shown in Figure 1. In contrast to AtVSR1 in wild-type plants, C2A:HA did not produce the high molecular mass 240-kD form in both Triton X-100- and CHAPS-treated protein samples (Fig. 6, B and C), confirming that C2A:HA is defective in the homomeric interaction.

Next, we examined the behavior of AtVSRs in C2A:HA transgenic plants using anti-AtVSR antibody. Fractions from the gel filtration column chromatography were analyzed by western blotting using anti-AtVSR antibody. In both Triton X-100- and CHAPS-treated samples, AtVSRs did not produce the high molecular mass forms around 240 kD (Fig. 6, B and C), indicating that C2A:HA interferes with the homomeric interaction of endogenous AtVSRs.

To confirm that C2A:HA does not form the high molecular mass form, fractions I, II, III, and IV from the gel filtration column chromatography were subjected to chemical cross-linking using DSP and then analyzed by western blotting using anti-HA antibody. In contrast to AtVSR1:HA, any of these fractions did not produce the high molecular mass form of C2A:HA (Fig. 6D), confirming that C2A:HA is defective in homomeric interaction in planta.

Next, we examined whether C2A:HA inhibits the vacuolar trafficking in transgenic plants. Protoplasts from the two C2A:HA transgenic lines were transformed with *Spo*:*GFP*, and its trafficking to the vacuole was examined by western-blot analysis using anti-GFP antibody. As a control, protoplasts from AtVSR1:HA transgenic plants were included in the analysis. Vacuolar trafficking of Spo:GFP in protoplasts of both C2A:HA transgenic lines was reduced to lower levels as compared with that in AtVSR1:HA protoplasts (Fig. 6E). These results confirmed that the homomeric interaction of AtVSR1 is critical for the vacuolar trafficking.

Localization of C2A:HA Is Different from That of Wild-Type AtVSR1

To gain an insight on how C2A caused the inhibition of vacuolar trafficking, we examined the location of C2A:HA in protoplasts. Previous studies demonstrated that the majority of AtVSR1 localizes to the PVC (Li et al., 2002; Kim et al., 2005; Miao et al., 2006). Consistent with these earlier observations, AtVSR1 closely overlapped with AtPEP12p:HA localized to the PVC but displayed only minor (11%) colocalization with SYP61 localized to the TGN (Fig. 7, A and C). Next, we examined the localization of C2A. Protoplasts were transformed with *C2A*:*Myc* and *AtPEP12p*:*HA*, a marker for the PVC (Sanderfoot et al., 1998), and then immunostained with anti-Myc and anti-HA antibodies. C2A:HA produced punctate staining patterns. However, a minor proportion (approximately 39%) of C2A:Myc-positive punctate stains overlapped with AtPEP12p:HA-positive punctate stains (Fig. 7, B and C), indicating that unlike wild-type AtVSR1, only a minor portion of C2A:HA localizes to the PVC. To further define its localization, *C2A*:*HA* was transformed into protoplasts together with *GmMan1*:*mRFP*, a marker localized to the cis-Golgi apparatus (Saint-Jore-Dupas et al., 2006), and their localization was compared by immunostaining using anti-HA antibody. GmMan1:mRFP was directly observed. A majority of C2A:HA-positive punctate stains localized side by side with those of GmMan1:mRFP (Fig. 7B), indicating that C2A:HA may localize to the trans-side of the Golgi apparatus, possibly the TGN. To test this possibility further, we compared the localization of C2A:HA with those detected by JIM84. JIM84 is a monoclonal antibody that detects a carbohydrate epitope localized to the Golgi apparatus (Fitchette et al., 1999; Jin et al., 2001). The major portion of C2A:HA localization was closely overlapped with those of JIM84 (Fig. 7B). We quantified the overlap between C2A:HA and JIM84, and approximately 61% of C2A:HA overlapped with those of JIM84-positive punctate stains (Fig. 7C), confirming that the majority of C2A:HA localizes to the Golgi apparatus, possibly the TGN. These results suggest that trafficking of C2A to the PVC is defective.

To confirm the localization of C2A, we examined the *N*-glycosylation pattern of C2A:HA. Protoplasts were transformed with *C2A*:*HA*, *AtVSR1*:*HA*, or *GKX* and then either left untreated or treated with tunicamycin, an inhibitor of *N*-glycosylation (Ericson et al., 1977; Lee et al., 2009). GKX is a chimeric ER-localized membrane protein consisting of the BiP leader sequence, an *N*-glycosylation motif (NLTD), the GFP-coding region, the TMD of the VSR of pea (*Pisum sativum*), and an ER retention motif (KKLL; Lee et al., 2009). Protein extracts were treated with or without endoglycosidase H (endo H) and analyzed by western blotting using anti-GFP antibody. As expected, AtVSR1:HA in tunicamycin-treated protoplasts migrated faster than that in protoplasts without tunicamycin treatment (Fig. 7D, panel a), indicating that AtVSR1:HA is *N*-glycosylated. Upon endo H treatment, the majority of both AtVSR1:HA and C2A:HA migrated at the same position as the endo H-untreated controls (Fig. 7D, panel b), indicating that both proteins have endo H-resistant *N*-glycans. In contrast, endo H-treated GKX migrated faster than non-endo H-treated GKX (Fig. 7D, panel c). These results together with the immunostaining results indicated that C2A:HA localizes to the Golgi apparatus or post-Golgi compartments.

To obtain supporting evidence that localization of C2A:HA is different from that of AtVSR1:HA, protein extracts from transgenic plants expressing AtVSR1:HA or C2A:HA were separated on a Suc density gradient by ultracentrifugation, and these fractions were analyzed by western blotting using anti-HA, anti-SYP21 (AtPEP12p), and anti-mannosidase I (anti-ManI) antibodies. SYP21 and ManI localize to the PVC and cis-Golgi, respectively. The majority of AtVSR1:HA comigrated with the PVC-localized SYP21 (Fig. 8). In addition, a minor portion comigrated with ManI. In contrast, the majority of C2A:HA was detected at lower Suc density positions than AtVSR1:HA (Fig. 8), indicating that the majority of C2A:HA did not localize to the PVC. These results strongly suggest that C2A:HA is defective in trafficking from the Golgi apparatus to the PVC.

C2A Fails to Form a Complex with Clathrin

The fact that C2A is defective in trafficking to the PVC raised the possibility that the mutant may not be incorporated into CCVs at the TGN. To test this possibility at the biochemical level, we determined the amount of AtVSR1 or C2A in CCV fractions. Total protein extracts from both transgenic plants, AtVSR1:

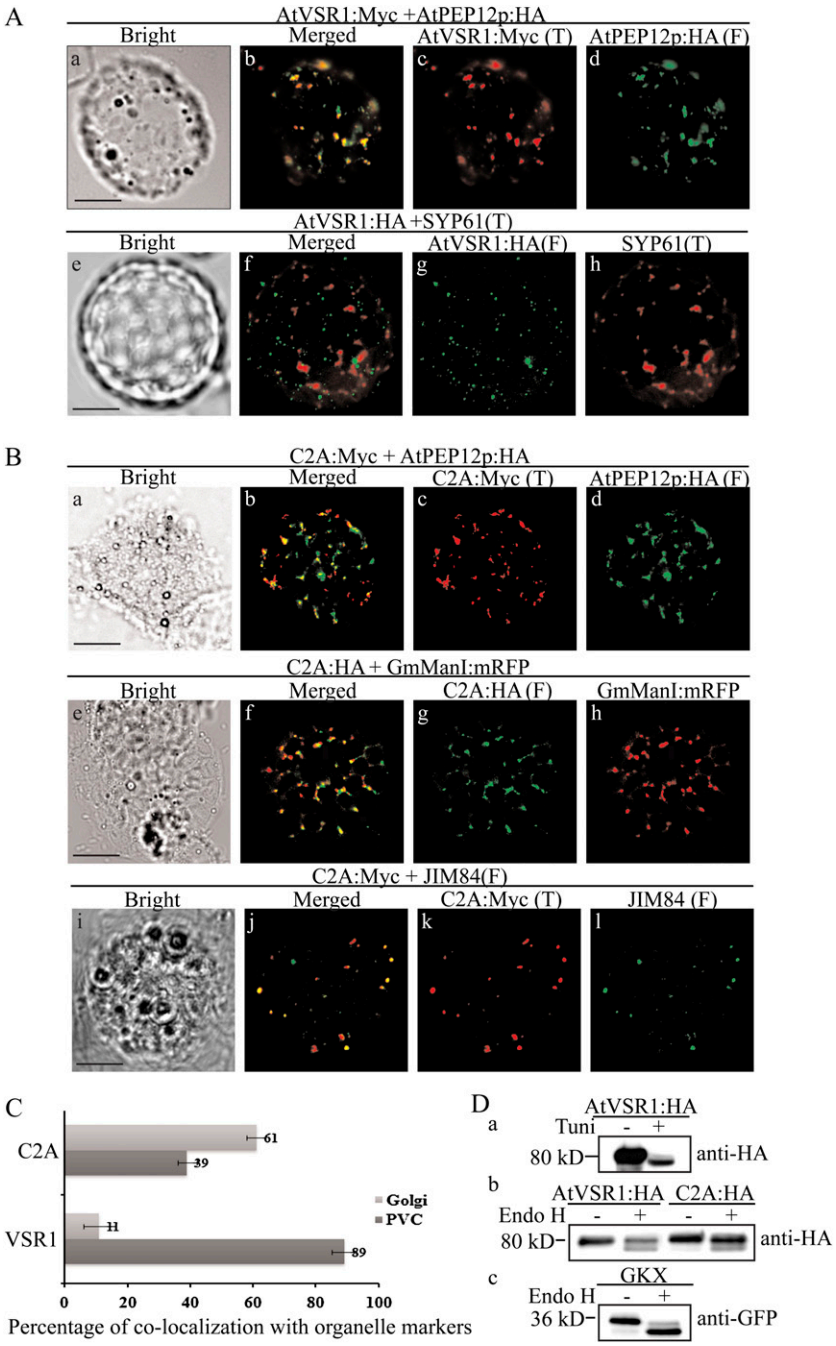

Figure 7. The majority of C2A:HA localizes to the TGN, with a minor proportion to the PVC. A and B, Localization of AtVSR1:Myc and C2A:Myc. Protoplasts were transformed with the indicated constructs, and localization of proteins was examined by immunostaining with the appropriate antibodies. The fluorescent signal of GmManI:mRFP was observed directly. F, Fluorescein isothiocyanate; T, tetramethylrhodamine-5-(and-6)-isothiocyanate. Bars = 20 μm. C, Quantification of overlap between C2A and organellar markers. The degree of overlap between C2A:Myc and JIM84 or AtPEP12p:HA was quantified by analyzing more than 50 protoplasts randomly selected from a population of transformed protoplasts each time. Three independent transformation experiments were performed. As a control, the degree of overlap between wild-type AtVSR1:Myc and organellar markers was quantified. Error bars indicate SD (n = 3). D, Endo H-resistant *N*-glycans of C2A:HA. Protoplasts transformed with the indicated constructs were incubated with or without tunicamycin (100 μg mL^{-1}) for 24 h, after which protein extracts were prepared from transformed protoplasts and treated with or without endo H. GKX was included as a control for ER proteins. The samples were analyzed by western blot using anti-HA or anti-GFP antibodies.

HA and C2A:HA, were fractionated by gel filtration column chromatography, and the high molecular mass fractions containing CCVs (fractions 1–6 in Fig. 1B) were pooled and used for immunoprecipitation using anti-HA antibody. The immunoprecipitates were analyzed by western blotting using an anti-HA antibody. In the immunoprecipitates, the amount of C2A:HA was reduced to 15% of that of AtVSR1:HA (Fig. 9), indicating that C2A:HA is not efficiently incorporated into CCVs. These results strongly suggested that the homomeric interaction is necessary for efficient interaction with adaptin of AP-1 at the TGN, which in turn is critical for CCV formation at the TGN for efficient vacuolar trafficking.

However, we cannot rule out the possibility that the mutant may have a defect in interaction with cargo proteins, which in turn results in failure to be incorporated into CCVs. We examined the binding affinity of C2A:HA to cargo proteins by coimmunoprecipitation. Protoplasts transformed with *AALP:GFP* together with *C2A:HA* or *AtVSR1:HA* were treated with latrunculin B to induce the accumulation of cargo proteins to the Golgi apparatus (Kim et al., 2005). As a negative control, we included AALPΔ(NPIR):GFP, which had a

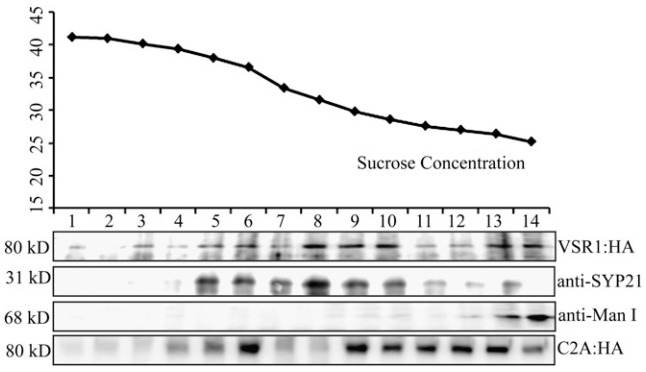

Figure 8. The distribution pattern of C2A:HA is different from that of AtVSR1 on a Suc gradient. Total protein extracts from transgenic plants expressing AtVSR1:HA or C2A:HA were fractionated on a continuous Suc density gradient by ultracentrifugation at 10,000*g* for 3 h, and each fraction was analyzed by western blotting using anti-HA, anti-ManI, and anti-SYP21 antibodies. The Suc density (w/v) was determined by a Suc refractometer.

deletion of the NPIR motif involved in the interaction with VSR. Subsequently, protein extracts prepared from transformed protoplasts were immunoprecipitated with anti-HA antibody and the precipitates were analyzed by western blotting using anti-GFP antibody. AALP:GFP was coprecipitated with both AtVSR1:HA and C2A:HA (Fig. 10A). In fact, the amount of AALP:GFP was higher in the C2A:HA precipitates than AtVSR1:HA precipitates. This is consistent with the localization pattern of the wild-type AtVSR1:HA and C2A:HA: the major portion of C2A:HA localized to the TGN, whereas only a minor portion of AtVSR1:HA localized at the TGN. The negative control, AALPΔ(NPIR):GFP, was not coprecipitated with either AtVSR1:HA or C2A:HA (Fig. 10B). These results suggest that the inhibitory effect of C2A on vacuolar trafficking is primarily due to inefficient incorporation of C2A to CCVs at the TGN.

DISCUSSION

In this study, we demonstrate that AtVSR1 forms high molecular mass complexes through homomeric interaction in vivo. This conclusion is based on the results obtained from gel filtration column chromatography and chemical cross-linking and coimmunoprecipitation experiments. Indeed, consistent with this hypothesis of the homomeric interaction, C2A:HA, an Ala substitution mutant that displayed a defect in homomeric interaction, not only failed to form high molecular mass forms among C2A:HA molecules but also interfered with the formation of high molecular mass forms of endogenous AtVSR1 in transgenic plants. This result raised the possibility that C2A:HA may act as a dominant negative mutant in the formation of high molecular mass forms through the homomeric interaction. Interestingly, expression of *C2A:HA* strongly induced endogenous *AtVSR1* in the transgenic plants. Often, a mutation in a gene causes induction of closely related isoforms as a mechanism to compensate for the mutation (Rosado et al., 2010). Thus, it is possible that expression of the dominant negative mutant *C2A:HA* might have caused expression of *AtVSR1* in the transgenic plants. At present, the exact composition of the high molecular mass complex is not known. The size of the high molecular mass strongly suggests that the 240-kD form may be either a homomeric trimer composed of only AtVSR1 or AtVSR isoforms or a complex composed of a dimer of AtVSR1 with an additional unidentified component(s). In leaf cells, highly homologous multiple AtVSR isoforms are known to be expressed (Miao et al., 2006). In the homomeric interaction of AtVSR1, both the TMD and CCD are necessary. However, the TMD of AtVSR1 can be replaced by the TMD from a heterologous protein, suggesting that the TMD may not have sequence-specific information but rather plays a structural role in the interaction between motifs in the CCD, such as anchoring AtVSR1 to the membrane. In contrast, the sequence information was contained in the CCD of AtVSR1. In the CCD of AtVSR1, a nine-amino acid region (C2 segment) that partly overlaps with the YMPL motif was found to be most critical for the interaction.

What would be the function of the AtVSR1 homomeric interaction? The high molecular mass complex containing multiple AtVSR1 molecules could function more efficiently as a sorting receptor in two ways. First, as a homocomplex, the effective concentration of the cargo-binding luminal domain is increased, thus facilitating the interaction between AtVSR1 and its cargo. This mechanism plays a critical role in the trafficking of phaseolin, a storage protein of the common bean (*Phaseolus vulgaris*). Phaseolin is targeted to the protein storage vacuole as a trimer, and the targeting efficiency is proportional to the number of C-terminal sorting signals in the trimer (Holkeri and Vitale, 2001). However, this possibility is rather remote, because the cargo-binding affinity of C2A:HA was not affected when examined by coimmunoprecipitation.

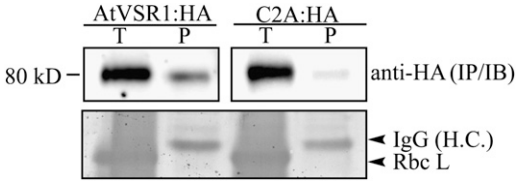

Figure 9. C2A:HA is not efficiently incorporated into CCVs. Total protein extracts from both transgenic plants, AtVSR1:HA and C2A:HA, were separated by gel filtration column chromatography in the presence of CHAPS as described for Figure 1B. The high molecular mass fractions containing CCVs (fraction numbers 1–6 in Fig. 1B) from gel filtration were pooled and subjected to immunoprecipitation using anti-HA antibody. Precipitates were analyzed by western-blot analysis with anti-HA antibody. IgG (H.C.), IgG heavy chain used as loading control; P, immunoprecipitates from the CCV fractions; RbcL, the large subunit of the Rubisco complex used as a loading control for the total protein extracts; T, total protein extracts of transformed protoplasts.

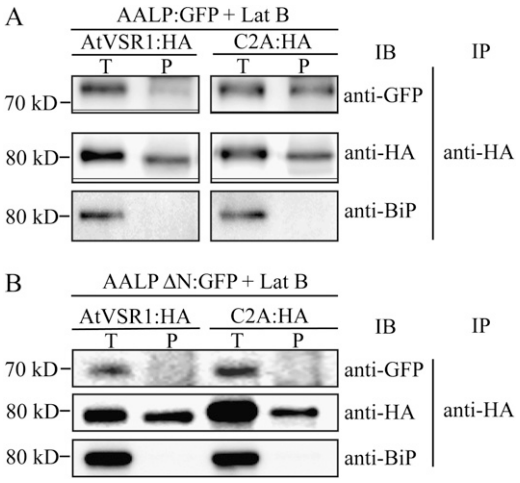

Figure 10. The Ala substitution of the C2A segment does not affect cargo binding. A, Protoplasts were transformed with the indicated constructs, incubated in the presence of latrunculin B (Lat B; 10 μM), and immunoprecipitated with anti-HA antibody. B, As a negative control, *AALP* without NPIR, the VSR-binding motif (AALPΔNPIR), was generated, fused to GFP, and transformed into protoplasts, and protein extracts were subjected to coimmunoprecipitation. Immunoprecipitates were analyzed by western-blot analysis with anti-HA, anti-GFP, and anti-BiP antibodies. IB, Western blot analysis; IP, immunoprecipitation; P, immunoprecipitates; T, total protein extracts of transformed protoplasts.

Another possibility is that the multiple CCDs of AtVSR1 in the complex could recruit accessory proteins more efficiently or act to stabilize the interaction of AtVSR1 with accessory proteins. These accessory proteins may include adaptor proteins such as AP-1 and EpsinR1 (Happel et al., 2004; Song et al., 2006). Pea VSR1 interacts with Arabidopsis μ-adaptin of the AP-1 complex through the YXXΦ motif in the C-terminal region of VSR1 (Happel et al., 2004). In addition, Arabidopsis EpsinR1 has been shown to interact with AtVSR1 and plays an important role in vacuolar trafficking of soluble proteins (Song et al., 2006). Thus, both of these adaptors may recruit clathrin to the TGN for cargo-bound AtVSR1. Indeed, Arabidopsis EpsinR1 has been shown to interact with clathrin, and also β1-adaptin of AP-1 in animal cells has been shown to interact with clathrin (Traub et al., 1995; Song et al., 2006). Interestingly, a previous study has shown that AP-1 undergoes oligomerization, which is advantageous for the formation of CCVs (Meyer et al., 2005). Moreover, the oligomerization of AP-1 was induced by a sorting signal of cargo proteins. The homomeric interaction of vacuolar sorting receptors could be in favor of the AP-1 polymerization. Similarly, yeast Vps41p, which is involved in the alkaline phosphatase pathway, undergoes oligomerization, and this is also thought to be a mechanism to promote vesicle formation (Darsow et al., 2001).

The hypothesis that homomeric interaction of AtVSR1 in the complex is in favor of CCV formation was tested by examining the amount of AtVSR1 or C2A cofractionated with CCVs. In agreement with this theory, the amount of C2A:HA cofractionated with CCVs was greatly reduced compared with that of the wild-type AtVSR1:HA. This was not due to a lack of C2A to the Gogli apparatus. In fact, the majority of C2A:HA localizes to the Golgi apparatus, in contrast to the wild-type AtVSR1 (Li et al., 2002; Kim et al., 2005; Miao et al., 2006). Since clathrin does not directly interact with AtVSR1, the smaller amount of C2A:HA in the CCV fraction is likely caused by a defect of C2A:HA in binding to adaptor proteins such as AP-1 and/or EpsinR1. C2A has a Y-to-A substitution in the YXXΦ motif that is involved in μ-adaptin binding. Therefore, we cannot exclude the possibility that C2A may have a defect in binding to μ-adaptin of AP-1, which in turn results in failure to be incorporated into CCVs efficiently. These results strongly argue for the hypothesis that the homomeric interaction is critical for a high-affinity binding to adaptor proteins, which in turn contributes to efficient recruitment of clathrin to the TGN.

The functional significance of the homomeric AtVSR1 interactions in the trafficking of vacuolar proteins was addressed in protoplasts. Overexpression of C2A:HA interfered with trafficking of both vacuolar proteins, AALP:GFP and Spo:GFP, and caused them to be secreted into the medium. In addition, C2A:HA expressed in transgenic plants also inhibited vacuolar trafficking of Spo:GFP. The inhibitory effect on the vacuolar trafficking was specific to C2A:HA. This conclusion is based on the fact that overexpression of wild-type AtVSR1:HA or C4A:HA, another C-terminal domain Ala substitution mutant, did not cause inhibition of vacuolar trafficking. However, this inhibitory effect of C2A:HA was relieved by a high level of wild-type AtVSR1:HA, suggesting that C2A:HA may act as a dominant negative mutant in the formation of high molecular mass complexes of AtVSR1. This hypothesis is consistent with the fact that endogenous *AtVSR1* was strongly induced in transgenic plants expressing *C2A:HA*. Thus, one possible scenario is that as C2A:HA fails to oligomerize and is not incorporated into CCVs, it is sent together with the cargo proteins to the plasma membrane, where cargoes bound to C2A:HA are released into medium.

Based on our results, we propose that the homomeric interaction between AtVSR1 molecules at the TGN plays a critical role in efficient recruitment of adaptor proteins to the TGN, which in turn is important for efficient recruitment of clathrin for CCV formation at the TGN during vacuolar trafficking in plant cells.

MATERIALS AND METHODS

Growth of Plants

Arabidopsis (*Arabidopsis thaliana* ecotype Columbia) was grown on B5 plates in a growth chamber at 20°C to 22°C under a 16-h/8-h light/dark cycle.

Leaf tissues were harvested from 1- to 2-week-old plants and immediately used for protoplast isolation.

Construction of Plasmid DNAs

AtVSR1 (Atg3g52850) was isolated by PCR from an Arabidopsis cDNA library using the specific primers VSR-5 and VSR-3 (Supplemental Table S1). To fuse HA and Myc to AtVSR1 at the C terminus, the AtVSR1 PCR product was reamplified with primers VSR-5/HA-3 and VSR-5/Myc-3, respectively. To generate AtVSR1ΔCCD:HA, PCR was carried out with primers VSR-5 and dC-3.

The AtVSR1 deletion and substitution mutants Lu, TS, CS, and TCS were generated by PCR using the following primers: VSR-5 and Lu-3 for Lu, TS-5 and TS-3 for TS, CS-5 and CS-3 for CS, and TCS-5 and TCS-3′ for TCS. To generate the Ala substitution mutants of C1A to C4A, PCR was performed using pairs of oligonucleotides corresponding to each of the mutated regions with 21 bases corresponding to sequences on either side of the mutated region. The primers were C1A-5 and C1A-3 for C1A, C2A-5 and C2A-3 for C2A, C3A-5 and C3A-3 for C3A, and C4A-5 and C4A-3 for C4A. The PCR products were fused to the HA or Myc tag and placed under the control of the cauliflower mosaic virus 35S promoter in pUC.

MBP:TCT:HA, MBP:TCT:Myc, and MBP:Myc were generated by PCR. The primer sets used were MTCT-5 and HA3-2 for MBP:TCT:HA, MTCT-5 and Myc3-2 for MBP:TCT:Myc, and MMyc-5 and MMyc-3 for MBP:Myc. The fidelity of all the PCR products was confirmed by nucleotide sequencing. These PCR products were ligated into pMAL-c2 (New England Biolabs) using *Eco*RI and *Xho*I sites.

The AALP(ΔNPIR) mutant was generated by PCR using primers DNPIR5 and DNPIR3. This PCR product was ligated into the N terminus of GFP using *Xba*I and *Bam*HI sites in a GFP-containing vector.

Transient Expression, Immunofluorescence Staining, and Microscopy

Plasmids were introduced by polyethylene glycol-mediated transformation (Jin et al., 2001). The expression of constructs was monitored at various time points after transformation. Images of GFPs in intact protoplasts were obtained from protoplasts in incubation medium on a glass slide covered with a coverslip. For immunostaining, transformed protoplasts were placed onto poly-L-Lys-coated glass slides and incubated in 3% paraformaldehyde in fixing buffer (10 mM HEPES [pH 7.4], 154 mM NaCl, 125 mM $CaCl_2$, 2.5 mM maltose, and 5 mM KCl) for 1 h at room temperature (Frigerio et al., 1998; Park et al., 2005). The fixed cells were incubated with rat monoclonal anti-HA, rabbit anti-Myc, or mouse anti-JIM84 antibodies at 4°C overnight and washed with TSW buffer (10 mM Tris-HCl [pH 7.4], 0.9% NaCl, 0.25% gelatin, 0.02% SDS, and 0.1% Triton X-100) three times. Subsequently, the cells were incubated with tetramethylrhodamine-5-(and-6)-isothiocyanate- or fluorescein isothiocyanate-conjugated goat anti-rabbit IgG (Sigma), anti-rat IgG (Zymed), and anti-rat IgM (Jackson ImmunoResearch Laboratories) secondary antibodies. The immunostained protoplasts were mounted in medium (100 mM Tris [pH 8.5] and 25% glycerol) containing Mowiol4-88 (Calbiochem). Images were taken with a fluorescence microscope (Axioplan 2; Carl Zeiss) equipped with a 40×/0.75 objective (Plan-NEOFLUAR) and a cooled CCD camera (Senicam; PCO Imaging) at 20°C. The filter sets used were XF116 (exciter, 474AF20; dichroic, 500DRLP; emitter, 510AF23) and XF117 (exciter, 540AF30; dichroic, 570DRLP; emitter, 585ALP; Omega Optical). Photoshop (version 7.0) was used to process the images.

Western-Blot Analysis and Suc Gradient

Cell extracts from protoplasts were prepared as described previously (Jin et al., 2001). To prepare proteins from the culture medium, cold TCA (100 μL) was added to the medium (1 mL) and protein aggregates were precipitated by centrifugation at 10,000*g* at 4°C for 5 min. Protein aggregates were dissolved in a solution of 0.1 N NaOH. Proteins were analyzed by western blot using anti-GFP and anti-HA (Roche Diagnostics) antibodies, as described previously (Jin et al., 2001).

Total protein extracts were fractionated by a continuous Suc density gradient by ultracentrifugation at 10,000*g* for 3 h (Kim et al., 2001; Oliviusson et al., 2006), and each fraction was analyzed by western blotting using appropriate antibodies.

Proteins were visualized using an ECL detection kit (Amersham Pharmacia Biotech), and images were obtained using an LAS3000 image-capture system (FujiFilm).

Coimmunoprecipitation and Cross-Linking of Proteins

Protein extracts prepared in immunoprecipitation buffer (25 mM HEPES [pH 6.8], 125 mM potassium acetate, 5 mM magnesium acetate, 1 mM $CaCl_2$, 1 mM dithiothreitol [DTT], 0.2 mM phenylmethylsulfonyl fluoride [PMSF], 0.2% [v/v] Triton X-100, and 0.2% [v/v] Nonidet P-40) supplemented with an EDTA-free protease inhibitor cocktail were precleared by incubating them with Protein A-Sepharose (CL-4B; Amersham) for 30 min, followed by centrifugation at 10,000*g* for 5 min at 4°C. Subsequently, 4 μg of anti-HA antibody (12CA5; Roche Diagnostics) was added to the precleared supernatants, and they were incubated for 3 h at 4°C. Immune complexes were purified by incubation with Protein A-Agarose for 1 h at 4°C. Purified complexes were washed three times with immunoprecipitation buffer, resuspended in homogenization buffer, and subjected to western-blot analysis.

For cross-linking, we used two different types of cross-linking agents, DSP and DTSSP. DSP was dissolved in dimethyl sulfoxide according to the manufacturer's instruction (22585; Pierce) and added to the protein samples in a buffer (25 mM HEPES [pH 6.8], 125 mM potassium acetate, 5 mM magnesium acetate, 1 mM $CaCl_2$, 1 mM DTT, 0.2 mM PMSF, 0.2% [v/v] Triton X-100, and 0.2% [v/v] Nonidet P-40) at 2 mM final concentration, and DTSSP was directly added to the protein samples at 2 mM final concentration. The reaction mixture was incubated on ice for 2 h, and the reaction was stopped with 1 M Tris-HCl (pH 7.5). Subsequently, the protein extracts were subjected to western-blot analysis or immunoprecipitation followed by western-blot analysis.

Gel Filtration Column Chromatography

Protein extracts were prepared in immunoprecipitation buffer (25 mM HEPES [pH 6.8], 125 mM potassium acetate, 5 mM magnesium acetate, 1 mM $CaCl_2$, 1 mM DTT, 0.2 mM PMSF, and 1% [v/v] Triton X-100 or 1% [v/v] CHAPS). Homogenates were centrifuged at 14,000*g* for 5 min and filtered with a microfilter (0.2 μm) to remove debris. The supernatant was applied to a Superdex 200 HR 10/30 column (Amersham Biosciences). Proteins were eluted with immunoprecipitation buffer at a flow rate of 0.5 mL min^{-1} with a fraction volume of 0.5 mL. Each fraction was subjected to western-blot analysis.

Expression of Recombinant Proteins and Protein Pull-Down Assay

MBP fusion protein constructs were introduced into *Escherichia coli* BL21 (DE3)LysS cells. Expression of recombinant proteins was induced by 0.7 mM isopropylthio-β-galactoside for 3 h at 28°C. Bacterial cultures were harvested by centrifugation at 5,000*g* for 5 min at 4°C, and cells were resuspended in ice-cold buffer (25 mM HEPES-KOH [pH 7.5], 150 mM NaCl, 1 mM EDTA, 1 mM dithiothreitol, and 1 mM PMSF) containing protease inhibitors (1 μg mL^{-1} aprotinin and 1 μg mL^{-1} antipain). The cells were lysed by sonication at 4°C. Cell debris was removed by centrifugation at 13,000*g* for 15 min at 4°C. Supernatants were then incubated with 1/100th volume of preequilibrated amylose resin on an orbital shaker for 1 h at 4°C. The beads were collected by centrifugation at 1,000*g* for 1 min and washed three times with ice-cold suspension buffer. Fusion proteins were eluted by adding 10 mM maltose in 50 mM Tris-HCl (pH 8.0).

To perform protein pull-down experiments, total protein extract from protoplasts was incubated with purified MBP fusion proteins or MBP alone that had been immobilized on amylose-Sepharose beads in binding buffer (25 mM HEPES-KOH [pH 7.5[, 150 mM NaCl, 1 mM EDTA, 1 mM dithiothreitol, and 1 mM PMSF) at 4°C for 2 h. Sepharose beads together with bound proteins were washed with ice-cold buffer three times. Sepharose-bound proteins were analyzed by western blotting using anti-HA and anti-Myc antibodies.

Endo H and Tunicamycin Treatment

Extracts were prepared from transformed protoplasts incubated in the presence or absence of tunicamycin (100 μg mL^{-1}) and treated with endo H (500 units) in 50 mM sodium citrate (pH 5.5). Protein extracts from each sample

were boiled in a denaturation buffer (2% SDS and 1 M β-mercaptoethanol) for 10 min and then incubated with endo H at 37°C for 1 h. The reactions were stopped by adding SDS-PAGE sample buffer and directly applied for western-blot analysis.

RT-PCR Analysis of Transcripts

For RT-PCR analysis, total RNA was isolated from 10-d-old seedlings grown on Murashige and Skoog plates using an RNeasy mini kit (Qiagen). RT was performed with 2 μg of total RNA using SuperScript II (Invitrogen) using random primers mixed with oligo(dT) primer at 42°C for 50 min and followed by heat inactivation of the reverse transcriptase at 70°C for 15 min. PCR was performed using ExTaq polymerase (Takara) at 94°C for 30 s, 50°C for 30 s, and 72°C for 30 s for 25 cycles using AtVSR1-specific primers (5′-ATGTGTTCGGGTTTTCAAGAGTCAACG-3′ and 5′-GATCCCTCTAATTTCCGCATCCATGTA-3′) and C2A-specific primers (5′-ATGTGTTCGGGTTTTCAAGAGTCAACG-3′ and 5′-GAACGATCGGGGAAATTC-3′). PCR products were visualized by ethidium bromide staining. 18S rRNA was included as an internal control for PCR. The primers for 18S rRNA were 5′-ATGATAACTCGACGGATCGC-3′ and 5′-CCTCCAATGGATCCTCGTTA-3′.

Sequence data from this article can be found in the GenBank/EMBL data libraries under accession number NP_190853.1 (AtVSR1).

Supplemental Data

The following materials are available in the online version of this article.

Supplemental Table S1. Primers used in this study.

Received May 23, 2010; accepted July 4, 2010; published July 12, 2010.

LITERATURE CITED

Ahmed SU, Bar-Peled M, Raikhel NV (1997) Cloning and subcellular location of an Arabidopsis receptor-like protein that shares common features with protein-sorting receptors of eukaryotic cells. Plant Physiol **114:** 325–336

Ahmed SU, Rojo E, Kovaleva V, Venkataraman S, Dombrowski JE, Matsuoka K, Raikhel NV (2000) The plant vacuolar sorting receptor AtELP is involved in transport of NH(2)-terminal propeptide-containing vacuolar proteins in *Arabidopsis thaliana*. J Cell Biol **149:** 1335–1344

Crowley KS, Liao S, Worrell VE, Reinhart GD, Johnson AE (1994) Secretory proteins move through the endoplasmic reticulum membrane via an aqueous, gated pore. Cell **78:** 461–471

Darsow T, Katzmann DJ, Cowles CR, Emr SD (2001) Vps41p function in the alkaline phosphatase pathway requires homo-oligomerization and interaction with AP-3 through two distinct domains. Mol Biol Cell **12:** 37–51

daSilva LL, Foresti O, Denecke J (2006) Targeting of the plant vacuolar sorting receptor BP80 is dependent on multiple sorting signals in the cytosolic tail. Plant Cell **18:** 1477–1497

daSilva LL, Taylor JP, Hadlington JL, Hanton SL, Snowden CJ, Fox SJ, Foresti O, Brandizzi F, Denecke J (2005) Receptor salvage from the prevacuolar compartment is essential for efficient vacuolar protein targeting. Plant Cell **17:** 132–148

Dennes A, Madsen P, Nielsen MS, Petersen CM, Pohlmann R (2002) The yeast Vps10p cytoplasmic tail mediates lysosomal sorting in mammalian cells and interacts with human GGAs. J Biol Chem **277:** 12288–12293

Dintzis SM, Velculescu VE, Pfeffer SR (1994) Receptor extracellular domains may contain trafficking information: studies of the 300-kDa mannose 6-phosphate receptor. J Biol Chem **269:** 12159–12166

Doray B, Ghosh P, Griffith J, Geuze HJ, Kornfeld S (2002) Cooperation of GGAs and AP-1 in packaging MPRs at the trans-Golgi network. Science **297:** 1700–1703

Ericson MC, Gafford JT, Elbein AD (1977) Tunicamycin inhibits GlcNAc-lipid formation in plants. J Biol Chem **252:** 7431–7433

Fitchette AC, Cabanes-Macheteau M, Marvin L, Martin B, Satiat-Jeunemaitre B, Gomord V, Crooks K, Lerouge P, Faye L, Hawes C (1999) Biosynthesis and immunolocalization of Lewis a-containing *N*-glycans in the plant cell. Plant Physiol **121:** 333–344

Frigerio L, de Virgilio M, Prada A, Faoro F, Vitale A (1998) Sorting of phaseolin to the vacuole is saturable and requires a short C-terminal peptide. Plant Cell **10:** 1031–1042

Gu F, Crump CM, Thomas G (2001) Trans-Golgi network sorting. Cell Mol Life Sci **58:** 1067–1084

Hadlington JL, Denecke J (2000) Sorting of soluble proteins in the secretory pathway of plants. Curr Opin Plant Biol **3:** 461–468

Happel N, Honing S, Neuhaus JM, Paris N, Robinson DG, Holstein SE (2004) Arabidopsis mu A-adaptin interacts with the tyrosine motif of the vacuolar sorting receptor VSR-PS1. Plant J **37:** 678–693

Harasaki K, Lubben NB, Harbour M, Taylor MJ, Robinson MS (2005) Sorting of major cargo glycoproteins into clathrin-coated vesicles. Traffic **6:** 1014–1026

Holkeri H, Vitale A (2001) Vacuolar sorting determinants within a plant storage protein trimer act cumulatively. Traffic **2:** 737–741

Honing S, Sosa M, Hille-Rehfeld A, von Figura K (1997) The 46-kDa mannose 6-phosphate receptor contains multiple binding sites for clathrin adaptor. J Biol Chem **272:** 19884–19890

Jin JB, Kim YA, Kim SJ, Lee SH, Kim DH, Cheong GW, Hwang I (2001) A new dynamin-like protein, ADL6, is involved in trafficking from the trans-Golgi network to the central vacuole in *Arabidopsis*. Plant Cell **13:** 1511–1526

Johnson KF, Kornfeld S (1992) The cytoplasmic tail of the mannose 6-phosphate/insulin-like growth factor-II receptor has two signals for lysosomal enzyme sorting in the Golgi. J Cell Biol **119:** 249–257

Kim H, Park M, Kim SJ, Hwang I (2005) Actin filaments play a critical role in vacuolar trafficking at the Golgi complex in plant cells. Plant Cell **17:** 888–902

Kim YW, Park DS, Park SC, Kim SH, Cheong GW, Hwang I (2001) Arabidopsis dynamin-like 2 that binds specifically to phosphatidylinositol 4-phosphate assembles into a high-molecular weight complex in vivo and in vitro. Plant Physiol **127:** 1243–1255

Kirsch T, Paris N, Butler JM, Beevers L, Rogers JC (1994) Purification and initial characterization of a potential plant vacuolar targeting receptor. Proc Natl Acad Sci USA **91:** 3403–3407

Kirsch T, Saalbach G, Raikhel NV, Beevers L (1996) Interaction of a potential vacuolar targeting receptor with amino- and carboxyl-terminal targeting determinants. Plant Physiol **111:** 469–474

Lee HK, Cho SK, Son O, Xu Z, Hwang I, Kim WT (2009) Drought stress-induced Rma1H1, a RING membrane-anchor E3 ubiquitin ligase homolog, regulates aquaporin levels via ubiquitination in transgenic *Arabidopsis* plants. Plant Cell **21:** 622–641

Lee MC, Miller EA, Goldberg J, Orci L, Schekman R (2004) Bi-directional protein transport between the ER and Golgi. Annu Rev Cell Dev Biol **20:** 87–123

Li YB, Rogers SW, Tse YC, Lo SW, Sun SS, Jauh GY, Jiang L (2002) BP-80 and homologs are concentrated on post-Golgi: probable lytic prevacuolar compartments. Plant Cell Physiol **43:** 726–742

Marcusson EG, Horazdovsky BF, Cereghino JL, Gharakhanian E, Emr SD (1994) The sorting receptor for carboxypeptidase Y is encoded by the VPS10 gene. Cell **77:** 579–586

Matsuoka K, Bassham DC, Raikhel NV, Nakamura K (1995) Different sensitivity to wortmannin of two vacuolar sorting signals indicates the presence of distinct sorting machineries in tobacco cells. J Cell Biol **130:** 1307–1318

Meyer DM, Crottet P, Maco B, Degtyar E, Cassel D, Spiess M (2005) Oligomerization and dissociation of AP-1 adaptors are regulated by cargo signals and by ArfGAP1-induced GTP hydrolysis. Mol Biol Cell **16:** 4745–4754

Miao Y, Yan PK, Kim H, Hwang I, Jiang L (2006) Localization of green fluorescent protein fusions with the seven Arabidopsis vacuolar sorting receptors to prevacuolar compartments in tobacco BY-2 cells. Plant Physiol **142:** 945–962

Nakatsu F, Ohno H (2003) Adaptor protein complexes as the key regulators of protein sorting in the post-Golgi network. Cell Struct Funct **28:** 419–429

Nothwehr SF, Ha SA, Bruinsma P (2000) Sorting of yeast membrane proteins into an endosome-to-Golgi pathway involves direct interaction of their cytosolic domains with Vps35p. J Cell Biol **151:** 297–310

Oliviusson P, Heinzerling O, Hillmer S, Hinz G, Tse YC, Jiang L, Robinson DG (2006) Plant retromer, localized to the prevacuolar compartment and microvesicles in *Arabidopsis*, may interact with vacuolar sorting receptors. Plant Cell **18:** 1239–1252

Paris N, Neuhaus JM (2002) BP-80 as a vacuolar sorting receptor. Plant Mol Biol **50:** 903–914

Park M, Lee D, Lee G-J, Hwang I (2005) AtRMR1 functions as a cargo receptor for protein trafficking to the protein storage vacuole. J Cell Biol **170:** 757–767

Puertollano R, Aguilar RC, Gorshkova I, Crouch RJ, Bonifacino JS (2001) Sorting of mannose 6-phosphate receptors mediated by the GGAs. Science **292:** 1712–1716

Rapoport TA, Rolls MM, Jungnickel B (1996) Approaching the mechanism of protein transport across the ER membrane. Curr Opin Cell Biol **8:** 499–504

Rosado A, Sohn EJ, Drakakaki G, Pan S, Swidergal A, Xiong Y, Kang BH, Bressan RA, Raikhel NV (2010) Auxin-mediated ribosomal biogenesis regulates vacuolar trafficking in *Arabidopsis*. Plant Cell **22:** 143–158

Saint-Jore-Dupas C, Nebenführ A, Boulaflous A, Follet-Gueye ML, Plasson C, Hawes C, Driouich A, Faye L, Gomord V (2006) Plant N-glycan processing enzymes employ different targeting mechanisms for their spatial arrangement along the secretory pathway. Plant Cell **18:** 3182–3200

Sanderfoot AA, Ahmed SU, Marty-Mazars D, Rapoport I, Kirchhausen T, Marty F, Raikhel NV (1998) A putative vacuolar cargo receptor partially colocalizes with AtPEP12p on a prevacuolar compartment in Arabidopsis roots. Proc Natl Acad Sci USA **95:** 9920–9925

Seaman MNJ, Marcusson EG, Cereghino JL, Emr SD (1997) Endosome to Golgi retrieval of the vacuolar protein sorting receptor, Vps10p, requires the function of VPS29: VPS30 and VPS35 gene products. J Cell Biol **137:** 79–92

Shimada T, Fuji K, Tamura K, Kondo M, Nishimura M, Hara-Nishimura I (2003) Vacuolar sorting receptor for seed storage proteins in Arabidopsis thaliana. Proc Natl Acad Sci USA **100:** 16095–16100

Sohn EJ, Kim ES, Zhao M, Kim SJ, Kim H, Kim YW, Lee YJ, Hillmer S, Sohn U, Jiang L, et al (2003) Rha1, an *Arabidopsis* Rab5 homolog, plays a critical role in the vacuolar trafficking of soluble cargo proteins. Plant Cell **15:** 1057–1070

Song J, Lee MH, Lee GJ, Yoo CM, Hwang I (2006) Epsin1 plays an important role in the vacuolar trafficking of soluble cargo proteins in plant cells via its interactions with clathrin, AP1, AtVTI11, and AtVSR1. Plant Cell **18:** 2258–2274

Tang BL, Wang Y, Ong YS, Hong W (2005) COPII and exit from the endoplasmic reticulum. Biochim Biophys Acta **1744:** 293–303

Traub LM (2005) Common principles in clathrin-mediated sorting at the Golgi and the plasma membrane. Biochim Biophys Acta **1744:** 415–437

Traub LM, Kornfeld S, Ungewickell E (1995) Different domains of the AP-1 adaptor complex are required for Golgi membrane binding and clathrin recruitment. J Biol Chem **270:** 4933–4942

Tse YC, Lam SK, Jiang L (2009) Organelle identification and characterization in plant cells: using a combinational approach of confocal immunofluorescence and electron microscope. J Plant Biol **52:** 1–8

Tse YC, Mo B, Hillmer S, Zhao M, Lo SW, Robinson DG, Jiang L (2004) Identification of multivesicular bodies as prevacuolar compartments in *Nicotiana tabacum* BY-2 cells. Plant Cell **16:** 672–693

Watanabe E, Shimada T, Tamura K, Matsushima R, Koumoto Y, Nishimura M, Hara-Nishimura I (2004) An ER-localized form of PV72, a seed-specific vacuolar sorting receptor, interferes the transport of an NPIR-containing proteinase in Arabidopsis leaves. Plant Cell Physiol **45:** 9–17

Zheng H, von Mollard GF, Kovaleva V, Stevens TH, Raikhel NV (1999) The plant vesicle-associated SNARE AtVTI1a likely mediates vesicle transport from the trans-Golgi network to the prevacuolar compartment. Mol Biol Cell **10:** 2251–2264